

Mamba-Based Ensemble learning for White Blood Cell Classification

Lewis Clifton¹, Xin Tian², Duangdao Palasuwan³, Phandee Watanaboonyongcharoen⁴,
Ponlapat Rojnuckarin⁵, Nantheera Anantrasirichai⁶

¹Computer Science, University of Bristol, UK, js21767@bristol.ac.uk

²Centre for Human Genetics, University of Oxford, UK, xin.tian@well.ox.ac.uk

³Oxidation in Red Cell Disorders Research Unit, Faculty of Allied Health Sciences, Chulalongkorn University, Thailand, nantadao@gmail.com

⁴Department of Laboratory Medicine, Faculty of Medicine, Chulalongkorn University, Thailand, phandee_lee@yahoo.com

⁵Excellence Center in Translational Hematology, Faculty of Medicine, Chulalongkorn University, Thailand, Ponlapat.R@Chula.ac.th

⁶Visual Information Laboratory, University of Bristol, UK, N.Anantrasirichai@bristol.ac.uk

Abstract—White blood cell (WBC) classification assists in assessing immune health and diagnosing various diseases, yet manual classification is labor-intensive and prone to inconsistencies. Recent advancements in deep learning have shown promise over traditional methods; however, challenges such as data imbalance and the computational demands of modern technologies, such as Transformer-based models which do not scale well with input size, limit their practical application. This paper introduces a novel framework that leverages Mamba models integrated with ensemble learning to improve WBC classification. Mamba models, known for their linear complexity, provide a scalable alternative to Transformer-based approaches, making them suitable for deployment in resource-constrained environments. Additionally, we introduce a new WBC dataset, Chula-WBC-8, for benchmarking. Our approach not only validates the effectiveness of Mamba models in this domain but also demonstrates their potential to significantly enhance classification efficiency without compromising accuracy. The source code can be found at <https://github.com/LewisClifton/Mamba-WBC-Classification>.

Index Terms—Image classification, white blood cell, microscopic image, ensemble learning, Mamba, Transformer

I. INTRODUCTION

Classifying white blood cell (WBC) types is crucial, primarily because different types of WBCs serve distinct functions in the immune response. Accurate classification provides insights into an individual's immune health, aids in diagnosing infections and diseases, and guides treatment.

Manual WBC classification is labor-intensive and requires specialized training, often leading to diagnostic inconsistencies due to the subjectivity of blood morphology and human factors such as fatigue or distraction [1]. Although automated systems integrated into blood imaging analyzers aim to improve efficiency, their accuracy is questionable; some WBC types are detected correctly less than 50% of the time, and the systems (e.g. DI-60) are costly [2]. Anecdotal and empirical evidence points to significant limitations of the DI-60 system, despite its contributions to workflow efficiency [2]–[5]. Notably, the DI-60 struggles with accurately classifying WBC abnormalities crucial for diagnosing conditions like leukemia [2]. Furthermore, while the DI-60's capabilities can support workflows in a supplementary role, they fall

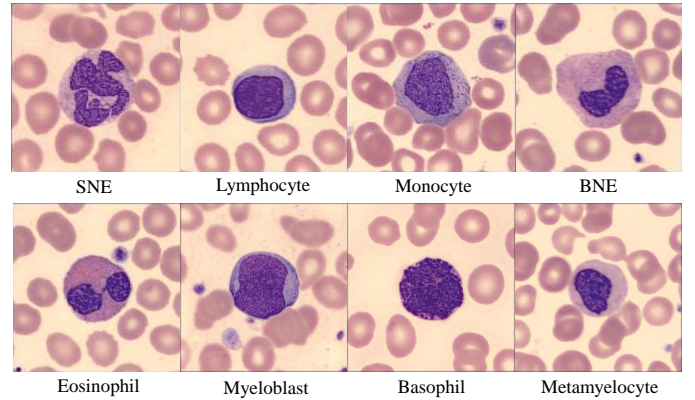


Fig. 1: Example images from the Chula-WBC-8 dataset of its eight WBC types: segmented neutrophils (SNE), lymphocytes, monocytes, band neutrophils (BNE), eosinophils, myeloblasts, basophils, and metamyelocytes in peripheral blood smears.

short without expert oversight [3], [4], ultimately increasing turnaround times, contradicting the intended benefits [5].

The emergence and development of new technology provide opportunities to address these limitations. Advances in Deep Learning (DL) have significantly enhanced WBC counting and differential classification, surpassing traditional approaches [6], [7]. More recently, Transformer architectures have been shown to be effective backbones for vision tasks. However, the attention mechanism attributed to the models' success suffers from quadratic complexity with respect to the input size, making them computationally expensive and difficult to deploy on hardware-constrained systems common in clinical laboratories [8].

This led to the proposal of Mamba [9], a model offering linear complexity as a scalable alternative in Transformer-dominated domains. Recent studies have demonstrated the effectiveness of Mamba-based models across various vision tasks [10]–[22]; however, the potential of Mamba remains unexplored for WBC classification.

Current DL based WBC classification suffers from several challenges in WBC classification such as dataset availabil-

ity, size and imbalance [23]. This arises due to the natural imbalance WBC subtypes in the blood and is a common problem among WBC datasets. Data imbalance causes bias towards majority classes, producing worse performance for rarer subtypes.

This paper proposes a novel framework based on Mamba models and their integration with ensemble learning for WBC classification. We also introduce a new WBC dataset (Fig. 1) to evaluate these models and address the emergent imbalance between WBC subtypes. The subsequent discussion of these results reveals the validity of Mamba as a tool in this domain and its potential to improve the efficiency of classification systems with minimal compromise to predictive accuracy. The main contributions of this paper can be summarized as follows:

- This paper presents the *first* use of Mamba models for WBC classification.
- Our novel framework is based on ensemble learning and integrates techniques for handling data imbalance.
- A new dataset, Chula-WBC-8, comprises eight types of WBCs from patients with WBC disorders.
- Comprehensive experiments comparing with Sysmex DI-60 and state-of-the-art deep learning approaches are conducted.

II. RELATED WORK AND BACKGROUND

A. Existing white blood cell classification methods

The initial application of DL for WBC classification utilized transfer learning, adapting models pre-trained on natural images using architectures such as VGG [24], ResNet, and Inception [25]. Later, advancements in the field introduced more sophisticated CNN-based models, such as DenseNet121 [26] and YOLO [27] to WBC classification. These architectures were specifically chosen for their capability to capture detailed and nuanced features of WBCs. Recent developments have integrated Transformer models and self-attention mechanisms, which excel in processing both local and global features within images [28]. This approach allows for more dynamic and context-aware feature analysis across the spatial domain of the images. Additionally, the integration of transformer-based object detection, such as DETR [29], introduces end-to-end training capabilities, significantly improving the precision and reliability of WBC classification.

B. Mamba

State Space Models (SSMs) map input sequences to output sequences through a latent state calculated from the previous state and current input, offering an efficient alternative to Transformers by scaling linearly with sequence length and enabling parallel computation. The Mamba frameworks utilize Structured State Space sequence model (S4) within a DL framework to manage long sequence states effectively. Mamba's selective scan mechanism updates parameters to determine which features of input tokens propagate forward. Its causal convolution blocks perform convolutions that are appropriate for sequences, reducing spatial dimensions of the input while ensuring that operations are limited to previous states. For visual data, input images are divided into spatially

encoded patches fed into a stack of Mamba blocks, which progressively down-sample feature maps to capture longer sequential dependencies in deeper blocks.

Mamba models for imaging tasks include several variants with distinct enhancements. Vision Mamba (Vim) [12] refines the standard Mamba block with a bidirectional approach and an extra branch for reverse convolution and reverse SSM networks to enhance global context representation. VMamba [11] applies Mamba to vision tasks using a novel 2D selective scan module that processes image patches from diverse scanning paths to generate detailed 2D feature maps. MambaVision [10] swaps causal convolution for standard convolution to allow richer context consideration by integrating both sequential and spatial dependencies. PlainMamba [14] maintains spatial adjacency and semantic continuity through a bi-directional scan path and directional encoding. LocalMamba [13] captures intra-region dependencies with local scans and a dual-branch attention mechanism for managing global and local feature interactions. MedMamba [15] incorporates grouped convolution for efficient feature capturing, showing high accuracy in tests like BloodMNIST [30] but remains underexplored for specific applications such as WBC classification, highlighting a significant area for future research [16].

III. DATASETS AND PREPARATION

This paper uses two datasets: BloodMNIST, an accessible benchmark for normal blood cell classification, and a newly introduced dataset, Chula-WBC-8, which contains cells from WBC disorders. The latter presents a greater challenge for automated classification.

A. BloodMNIST

BloodMNIST, part of the MedMNIST dataset [31], comprises 17,092 microscopic images of normal cells from healthy individuals free of infections, hematologic or oncologic diseases, and pharmacological treatments at the time of collection. The dataset is organized into 8 classes: neutrophils, eosinophils, basophils, lymphocytes, monocytes, immature granulocytes (promyelocytes, myelocytes, and metamyelocytes), erythroblasts and platelets or thrombocytes. As per the original paper, it is pre-partitioned into training, validation, and test sets in a 7:1:2 ratio. Initially, the images have a resolution of 360×363 pixels; they are center-cropped to 200×200 and subsequently resized to 28×28 pixels.

B. Chula-WBC-8

We collected 4,808 images of peripheral blood smears (Table I) using a Sysmex DI-60 machine from a sample group of 113 patients with WBC disorders at Chulalongkorn Hospital, Thai Red Cross Society. The types of WBCs from the peripheral blood smears were identified by five experts in a blind test, with the majority opinion, which is three out of five, used to confirm the answers. All WBC images were anonymized to ensure patient privacy. Table I shows the class frequencies for the dataset. The dataset exhibits significant inter-class imbalance, a common issue in WBC datasets due to the natural variation in WBC subtype prevalence.

TABLE I: Chula-WBC-8 dataset with class frequencies and augmentation details

Class	Original	Augmented	Total
SNE	1985	0	1985
Lymphocyte	1253	0	1253
Monocyte	567	0	567
BNE	514	86	500
Eosinophil	157	343	500
Myeloblast	156	344	500
Basophil	93	407	500
Metamyelocyte	83	417	500
Total:	4808	1607	6215

IV. METHODOLOGY

The proposed diagram is shown in Fig. 2, combining five Mamba-based models using ensemble learning.

A. Mamba architectures

Five Mamba-based methods are employed in our study, including Vision Mamba (ViM), VMamba [11], MambaVision [10], MedMamba [15], and LocalMamba [13].

1) *Vision Mamba (ViM)* [12]: A bi-directional version of the standard Mamba block is employed with the introduction of a third branch that uses reverse convolution and reverse SSM networks. This addition gives ViM a stronger representation of the global context of the input.

2) *VMamba* [11]: A novel 2D selective scan (SS2D) module is proposed. It forms four sequences of image patches obtained by traversing different scanning paths over the input patches. These are fed into independent S6 blocks (selective SSM) and cross-merged to produce a 2D feature map. The stacking of SS2D produces more granular feature maps deeper in the network, capturing finer details.

3) *MambaVision* [10]: swaps the causal convolution layer used by conventional Mamba with standard convolution to remove the restriction of considering the state sequence in one direction, which is inappropriate given the spatial nature of images. A second convolution layer is used in the secondary path, developing a richer global context by considering both sequential and spatial dependencies of the input in both paths of the block.

4) *LocalMamba* [13]: Local scans in four parallel directions capture intra-region dependencies and global interactions, employing a dual-branch attention mechanism. The spatial branch aggregates global information, while the channel branch adjusts token importance. This method captures detailed local and global features and dynamically optimizes scan paths for each layer, ensuring efficient feature prioritization and comprehensive interaction analysis.

5) *MedMamba* [15]: The modified VMamba block incorporates a grouped convolution layer in its secondary branch to efficiently capture a broad spectrum of features. Grouped convolutions require a channel-shuffle layer to facilitate feature integration and prevent information loss between channels. This setup enhances feature representation by combining sequential and spatial dependencies.

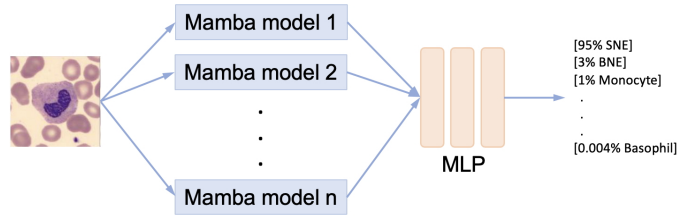


Fig. 2: Diagram of the proposed Mamba-based ensemble learning framework (n=5 in this paper).

B. Ensemble learning

Ensembles benefit from leveraging diverse base models to maximize variance, combining the predictions of several trained models through a “meta-learner” to enhance performance. In this paper, our training set is partitioned into two subsets: one for training base Mamba models and the other as a holdout set for training the meta-learner, preventing data leakage and ensuring that the training metrics for the meta-learner remain optimistic. While training the meta-learner, the base models generate predictions on the holdout data; these predictions are then concatenated as input for the meta-learner. The meta-learner is a simple Multilayer Perceptron (MLP) trained for 5 epochs to avoid overfitting, optimizing its ability to effectively integrate insights from the base models without inheriting their biases or specific errors.

C. Dealing with imbalanced dataset

We employ data augmentation and a weighted loss function to deal with imbalanced dataset.

The data augmentation applied includes random rotation (0° to 360°), translation ($\pm 10\%$ along both x and y axes), scaling (90% to 110%), and shearing ($\pm 5^\circ$). Horizontal and vertical flips are performed with a 50% probability each. Brightness and contrast are adjusted within $\pm 10\%$, saturation within $\pm 5\%$, and hue within $\pm 2\%$. Additionally, Gaussian blur is applied with a kernel size of 3 and sigma ranging from 0.1 to 1.0. Table I shows the resulting class frequencies following data augmentation for Chula-WBC-8 dataset.

In initial training phase, the original models utilize a cross-entropy loss function, which is standard for classification tasks. To further address class imbalance, we employ a weighted cross-entropy loss, assigning weights inversely proportional to the class frequencies, thus emphasizing minority classes.

D. Training settings

All models are trained using the AdamW optimizer. The training configuration for each model follows the settings specified in the original papers. The training was done using a single Nvidia RTX 4070 GPU.

The datasets used in this study are divided into training and test splits. The BloodMNIST dataset follows its predefined split, with 11,959 images for training, 1712 for validation, and 3,421 for testing. The Chula-WBC-8 dataset is partitioned using a 4:1 ratio for training and testing, respectively. Images

TABLE II: Performance of the models on BloodMNIST. **Bold** and underline indicate the best and second best performers.

Method	Acc.	F1	Prec.	Sens
ResNet-50 [31]	95.0%	-	-	-
Google AutoML [31]	96.6%	-	-	-
Without Imbalanced Data Strategy				
SWIN ViT [32]	98.80%	0.9880	0.9880	0.9880
VMamba [11]	98.91%	0.9891	0.9892	0.9892
Vim [12]	98.45%	0.9845	0.9847	0.9845
Medmamba [15]	94.48%	0.9446	0.9490	0.9448
MambaVision [10]	98.80%	0.9880	0.9880	0.9880
LocalMamba [13]	<u>99.04%</u>	<u>0.9904</u>	<u>0.9904</u>	<u>0.9904</u>
Ensemble(ours)	99.24%	0.9925	0.9924	0.9924
With Imbalanced Data Strategy				
SWIN ViT [32]	98.42%	0.9843	0.9850	0.9842
VMamba [11]	97.75%	0.9776	0.9781	0.9775
Vim [12]	98.71%	0.9871	0.9872	0.9871
Medmamba [15]	91.14%	0.9081	0.9299	0.9114
MambaVision [10]	<u>98.91%</u>	<u>0.9892</u>	<u>0.9892</u>	<u>0.9892</u>
LocalMamba [13]	98.36%	0.9836	0.9838	0.9836
Ensemble(ours)	99.12%	0.9912	0.9914	0.9912

are resized to 224×224 and normalized prior to being fed to the model.

V. EXPERIMENTAL RESULTS AND DISCUSSION

A. Evaluation Metrics

Model performance is evaluated using standard classification metrics: Accuracy (Acc.), Precision (Prec.), Sensitivity (Sens.), and F1 Score (F1). Accuracy quantifies the proportion of correctly classified samples, Precision indicates the fraction of predicted positives that are correct, Sensitivity measures the fraction of actual positives identified, and F1 provides their harmonic mean. Given the class imbalance, we report weighted averages for all metrics.

B. Results of BloodMNIST dataset

Table II presents the results of WBC classification. Mamba models outperform Google AutoML, the top benchmark in [31] by 2.7%. The BloodMNIST dataset does not display a significantly skewed distribution, resulting in minimal differences in performance between models trained with and without an imbalance strategy. Notably, Medmamba produced the poorest results, likely because we did not have access to the pretrained model, necessitating training from scratch. In contrast, LocalMamba and MambaVision are the top performers among individual models. Our ensemble learning approach did not yield significant improvement, as the overall performance on the BloodMNIST dataset was already high, indicating that all models are generally effective.

C. Results of Chula-WBC-8 dataset

Table III shows the results of Sysmex DI-60 WBC classification, and DL models both with and without adjustments for data imbalance. Given the imbalanced nature of this dataset, improvements are evident when strategies to address imbalance are employed in most models, except for the ensemble model. This might be that ensembling could naturally

TABLE III: Performance of the models on Chula-WBC-8. **Bold** and underline indicate the best and second best performers.

Method	Acc.	F1	Prec.	Sens
Sysmex DI-60	85.68%	0.9013	0.9720	0.8568
Without Imbalanced Data Strategy				
SWIN ViT [32]	<u>92.69%</u>	<u>0.9265</u>	<u>0.9263</u>	<u>0.9269</u>
VMamba [11]	91.95%	0.9212	0.9241	0.9195
Vim [12]	88.71%	0.8938	0.9092	0.8871
Medmamba [15]	65.83%	0.7625	0.6583	0.6684
MambaVision [10]	90.80%	0.9126	0.9080	0.9097
LocalMamba [13]	90.80%	0.9170	0.9080	0.9105
Ensemble (ours)	93.94%	0.9397	0.9401	0.9393
With Imbalanced Data Strategy				
SWIN ViT [32]	91.12%	0.9087	0.9114	0.9112
VMamba [11]	87.15%	0.8824	0.9190	0.8715
Vim [12]	89.66%	0.8921	0.8949	0.8966
Medmamba [15]	87.04%	0.8454	0.8533	0.8704
MambaVision [10]	92.00%	0.9186	0.9192	0.9192
LocalMamba [13]	92.79%	0.9272	0.9269	0.9279
Ensemble (ours)	<u>92.37%</u>	<u>0.9202</u>	<u>0.9199</u>	<u>0.9237</u>

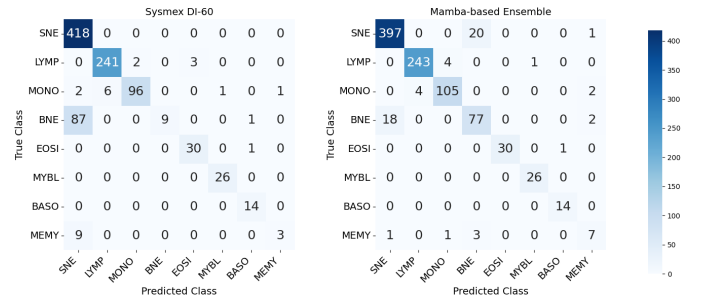


Fig. 3: Comparison of confusion matrices: Sysmex DI-60 (left) vs. Mamba-based ensemble learning (right).

overcome the imbalance issue. The Mamba models outperform DI-60 by up to 9.6%.

Fig. 3 compares the confusion matrix results from the Sysmex DI-60 and our Mamba-based ensemble learning approach. Both methods predominantly misclassify between SNE (segmented neutrophils) and BNE (band neutrophils), often due to some cells being in a transitional stage from BNE to SNE, resulting in ambiguous classifications. This comparison highlights both the challenges and the effectiveness of our model in handling classes with overlapping characteristics.

Fig. 4 shows the heatmap where key features are used for decision-making. Mamba focuses more on the cell area than Swin Transformer.

Overall performance is lower on Chula than on BloodMNIST because Chula has lower inter-class variance, making it more difficult to distinguish between classes. Chula contains only WBCs, whereas BloodMNIST includes WBCs, RBCs, and platelets, leading to greater variation in the dataset.

VI. CONCLUSION

This paper presents a new framework for WBC classification. We employ modern architectures, specifically Mamba,

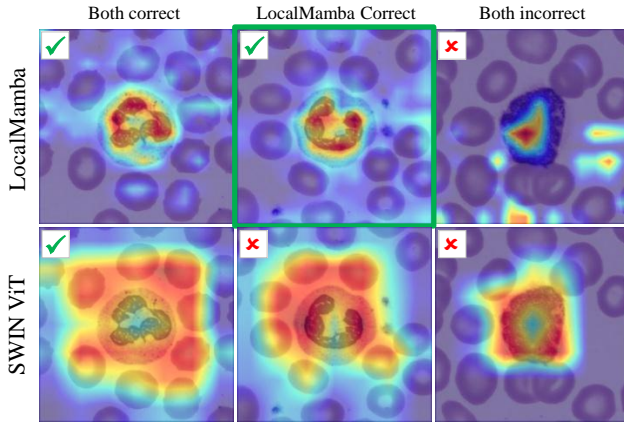


Fig. 4: Heatmap visualizations of key features (red indicates higher importance) across scenarios: (Left) Both correct, (Middle) Only LocalMamba correct, (Right) Both incorrect. Rows: LocalMamba (top), Swin Transformer (bottom).

and leverage ensemble learning to enhance overall performance. Additionally, we introduce a new dataset containing eight types of WBCs from patients with disorders. To address dataset imbalance, we apply data augmentation and a weighted loss function. The results demonstrate that our method outperforms CNNs, Swin Transformer and the automated software provided by Sysmex DI-60.

Future research could consider these downstream tasks, supplementing our own work to form a comprehensive overview of the potential of Mamba-based models in WBC tasks as well as potentially enabling an alternate approach to WBC-based diagnostics, such as automated Leukaemia detection.

REFERENCES

- [1] X. Fuentes-Arderiu, M. García-Panyella, and D. Dot-Bach, "Between-examiner reproducibility in manual differential leukocyte counting," *Accreditation and quality assurance*, vol. 12, pp. 643–645, 2007.
- [2] Y. Zhao, Y. Diao, J. Zheng, X. Li, and H. Luan, "Performance evaluation of the digital morphology analyzer sysmex di-60 for white blood cell differentials in abnormal samples," *Scientific Reports*, vol. 14, no. 1, p. 14344, 2024.
- [3] H. N. Kim, M. Hur, H. Kim, S. W. Kim, H.-W. Moon, and Y.-M. Yun, "Performance of automated digital cell imaging analyzer sysmex di-60," *Clinical Chemistry and Laboratory Medicine (CCLM)*, vol. 56, no. 1, pp. 94–102, 2018.
- [4] Y. Tabe, T. Yamamoto, I. Maenou, R. Nakai, M. Idei, T. Horii, T. Miida, and A. Ohsaka, "Performance evaluation of the digital cell imaging analyzer di-60 integrated into the fully automated sysmex xn hematology analyzer system," *Clinical Chemistry and Laboratory Medicine (CCLM)*, vol. 53, no. 2, pp. 281–289, 2015.
- [5] M. Nam, S. Yoon, M. Hur, G. H. Lee, H. Kim, M. Park, and H. N. Kim, "Digital morphology analyzer sysmex di-60 vs. manual counting for white blood cell differentials in leukopenic samples: a comparative assessment of risk and turnaround time," *Annals of laboratory medicine*, vol. 42, no. 4, pp. 398–405, 2022.
- [6] A.-D. Khamael, J. Banks, K. Nguyen, A. Al-Sabaawi, I. Tomeo-Reyes, and V. Chandran, "Segmentation of white blood cell, nucleus and cytoplasm in digital haematology microscope images: A review—challenges, current and future potential techniques," *IEEE Reviews in Biomedical Engineering*, vol. 14, pp. 290–306, 2020.
- [7] S. Han, H. Mao, and W. J. Dally, "Deep compression: Compressing deep neural networks with pruning, trained quantization and Huffman coding," *arXiv preprint arXiv:1510.00149*, 2015.
- [8] A. Shah, S. S. Naqvi, K. Naveed, N. Salem, M. A. Khan, and K. S. Alimgeer, "Automated diagnosis of leukemia: a comprehensive review," *IEEE Access*, vol. 9, pp. 132 097–132 124, 2021.
- [9] A. Gu and T. Dao, "Mamba: Linear-time sequence modeling with selective state spaces," *arXiv preprint arXiv:2312.00752*, 2023.
- [10] A. Hatamizadeh and J. Kautz, "Mambavision: A hybrid mamba-transformer vision backbone," *arXiv preprint arXiv:2407.08083*, 2024.
- [11] Y. Liu, Y. Tian, Y. Zhao, H. Yu, L. Xie, Y. Wang, Q. Ye, and Y. Liu, "Vmamba: Visual state space model," *arXiv:2401.10166*, 2024.
- [12] L. Zhu, B. Liao, Q. Zhang, X. Wang, W. Liu, and X. Wang, "Vision mamba: Efficient visual representation learning with bidirectional state space model," *arXiv preprint arXiv:2401.09417*, 2024.
- [13] T. Huang, X. Pei, S. You, F. Wang, C. Qian, and C. Xu, "Localmamba: Visual state space model with windowed selective scan," *arXiv preprint arXiv:2403.09338*, 2024.
- [14] C. Yang, Z. Chen, M. Espinosa, L. Ericsson, Z. Wang, J. Liu, and E. J. Crowley, "Plainmamba: Improving non-hierarchical mamba in visual recognition," *arXiv preprint arXiv:2403.17695*, 2024.
- [15] Y. Yue and Z. Li, "Medmamba: Vision mamba for medical image classification," *arXiv preprint arXiv:2403.03849*, 2024.
- [16] S. Bansal, S. Madisetty, M. Z. U. Rehman, C. S. Raghaw, G. Duggal, N. Kumar *et al.*, "A comprehensive survey of mamba architectures for medical image analysis: Classification, segmentation, restoration and beyond," *arXiv preprint arXiv:2410.02362*, 2024.
- [17] F. Ibrahim, G. Liu, and G. Wang, "A survey on mamba architecture for vision applications," *arXiv preprint arXiv:2502.07161*, 2025.
- [18] X. Liu, C. Zhang, and L. Zhang, "Vision mamba: A comprehensive survey and taxonomy," *arXiv preprint arXiv:2405.04404*, 2024.
- [19] H. Qu, L. Ning, R. An, W. Fan, T. Derr, H. Liu, X. Xu, and Q. Li, "A survey of mamba," *arXiv preprint arXiv:2408.01129*, 2024.
- [20] M. M. Rahman, A. A. Tutul, A. Nath, L. Laishram, S. K. Jung, and T. Hammond, "Mamba in vision: A comprehensive survey of techniques and applications," *arXiv preprint arXiv:2410.03105*, 2024.
- [21] R. Xu, S. Yang, Y. Wang, Y. Cai, B. Du, and H. Chen, "Visual mamba: A survey and new outlooks," *arXiv preprint arXiv:2404.18861*, 2024.
- [22] H. Zhang, Y. Zhu, D. Wang, L. Zhang, T. Chen, Z. Wang, and Z. Ye, "A survey on visual mamba," *Applied Sciences*, vol. 14, no. 13, p. 5683, 2024.
- [23] R. Asghar, S. Kumar, P. Hynds, and A. Shaukat, "Classification of white blood cells using machine and deep learning models: a systematic review," *CoRR*, 2023.
- [24] F. Özyurt, "A fused cnn model for wbc detection with mrmr feature selection and extreme learning machine," *Soft Computing*, vol. 24, pp. 8163–8172, 2020.
- [25] M. Habibzadeh, M. Jannesari, Z. Rezaei, H. Baharvand, and M. Totonchi, "Automatic white blood cell classification using pre-trained deep learning models: Resnet and inception," in *Tenth International Conference on Machine Vision*, vol. 10696, 2017, p. 1069612.
- [26] S. Sharma, S. Gupta, D. Gupta *et al.*, "Deep learning model for the automatic classification of white blood cells," *Computational Intelligence and Neuroscience*, vol. 2023, no. 1, 2023.
- [27] S. M. Abas, A. M. Abdulazeez, and D. Q. Zeebaree, "A yolo and convolutional neural network for the detection and classification of leukocytes in leukemia," *Indonesian Journal of Electrical Engineering and Computer Science*, vol. 25, no. 1, January 2022. [Online]. Available: <http://ijeecs.iaescore.com>
- [28] O. Katar and O. Yildirim, "An explainable vision transformer model based white blood cells classification and localization," *Diagnostics*, vol. 13, p. 2459, 2023.
- [29] B. Leng, C. Wang, M. Leng, M. Ge, and W. Dong, "Deep learning detection network for peripheral blood leukocytes based on improved detection transformer," *Biomedical Signal Processing and Control*, vol. 82, p. 104518, 2023.
- [30] J. Yang, R. Shi, and B. Ni, "Medmnist classification decathlon: A lightweight autml benchmark for medical image analysis," in *IEEE 18th International Symposium on Biomedical Imaging (ISBI)*, 2021, pp. 191–195.
- [31] J. Yang, R. Shi, D. Wei, Z. Liu, L. Zhao, B. Ke, H. Pfister, and B. Ni, "MedMNIST v2-A large-scale lightweight benchmark for 2d and 3d biomedical image classification," *Scientific Data*, vol. 10, no. 1, 2023.
- [32] Z. Liu, Y. Lin, Y. Cao, H. Hu, Y. Wei, Z. Zhang, S. Lin, and B. Guo, "Swin transformer: Hierarchical vision transformer using shifted windows," in *Proceedings of the IEEE/CVF international conference on computer vision*, 2021, pp. 10 012–10 022.